

An Improved Clutter Filtering and Spectral Moment Estimation Algorithm for Staggered PRT Sequences

M. SACHIDANANDA

Indian Institute of Technology, Kanpur, India

D. S. ZRNIC

National Severe Storms Laboratory, Norman, Oklahoma

(Manuscript received 13 July 2001, in final form 20 June 2002)

ABSTRACT

In the staggered pulse repetition time (PRT) radar, the phase difference between the autocorrelations at lag T_1 and T_2 is used for velocity estimation. This paper investigates velocity estimates from the autocorrelation at shorter lag, while the longer lag is used to resolve the ambiguity. This velocity estimate is shown to have lower error than the one using the phase difference. This method is preferred in the absence of ground clutter.

In a recent paper on the spectral processing of the staggered PRT sequences, a new algorithm was presented that enables the recovery of spectral moments in presence of ground clutter. Although this algorithm recovers velocity over the extended unambiguous interval corresponding to the difference PRT, there is a small bias error in the velocity and spectrum width estimates due to the loss of some of the signal components in the process of filtering the clutter. An enhancement in the algorithm is suggested that enables removal of this bias by reconstructing the lost spectral components before the spectral moments are estimated. The proposed algorithm completely removes the bias error in the velocity and spectral width most of the time thereby significantly improving these estimates.

The window function and the number of samples used for processing significantly influence the performance of the clutter filter. The window function effect is explored via simulation, and these results are presented.

1. Introduction

Sachidananda and Zrnic (2000) have suggested a new approach to clutter filtering and spectral moment estimation for the staggered pulse repetition time (PRT) radar scheme that eliminates the dropout regions in the unambiguous velocity interval and also significantly improves the estimate variance. In this method T_1 and T_2 are chosen such that they are integer multiples of a basic period T_u , so that an equivalent uniform sample sequence (with PRT T_u) can be constructed with a value zero assigned to missing samples. An important property of this reconstructed time series concerns its spectrum whereby the clutter coefficients spread over a small set of discrete regions so that their positions are exactly known. Hence the clutter can be filtered in the spectral domain. Of course, in the process, any signal present in these coefficients also will be removed. Nonetheless, a significant amount of the signal power is retained in the spectrum because the ground clutter generally has a very narrow spectrum compared to the signal. Thus,

the residual signal-to-clutter power ratio can be made larger than unity by appropriate selection of the clutter filter width, even if the signal and clutter spectra overlap significantly. The residual signal is then reconstructed using a magnitude deconvolution procedure. The velocity estimated from this reconstructed signal spectrum has a small bias because some of the signal spectral coefficients are deleted by the clutter filter. The bias becomes appreciable for wide clutter filters. The width of the clutter filter that produces a residual clutter-to-signal ratio (CSR) less than 0 dB depends on the CSR before clutter filtering, the mean velocity, and the width of the signal. A clutter-filtering and spectral-moment estimation algorithm is presented by Sachidananda and Zrnic (2000), where the clutter filtering is a more complex procedure than simple dropping of the clutter spectral coefficients. Although just dropping the coefficients would produce velocity estimates with similar bias, the bias correction requires the complex filtering procedure explained in that paper. The indicated clutter filtering scheme is used to retain a part of the signal power while the clutter is filtered out completely from the coefficients within the width of the clutter filter.

In this paper we further refine this clutter filtering

Corresponding author address: Dr. D. S. Zrnic, National Severe Storms Laboratory, 1313 Halley Circle, Norman, OK 73069.
E-mail: dusan.zrnic@nssl.noaa.gov

algorithm to recover the lost signal components and to remove the small bias present in all three spectral moment estimates. In the next section we briefly explain the earlier algorithm (Sachidananda and Zrnic 2000). Then we present two approaches for bias removal by way of restoring the lost signal components and some results from simulation studies.

An additional point brought out in this paper concerns velocity estimation in the absence of clutter. This is important because clutter is present mostly at close range, and the rest of the area on the radar display is typically free of clutter. In the absence of clutter it is best to use pulse pair type estimation, rather than the fast Fourier transform (FFT)-based estimation, because it gives unbiased estimates, and it is possible to compute velocity from R_1 , and use R_2 only to de-alias the velocity estimate (Sirmans et al. 1976).

For the most part we use the same mathematical notation as in our earlier paper (Sachidananda and Zrnic 2000), except when new parameters are introduced. Subscripted capital letters denote spectral coefficients, and lower-case letters the corresponding time-domain quantities. Boldface fonts represent matrices. We also frequently refer to the equations and figures in that paper.

2. Processing of the staggered PRT sequence

In the staggered PRT technique (Zrnic and Mahapatra 1985), two different pulse spacings, T_1 and T_2 , are used alternately to obtain autocorrelations, $R(T_1)$ and $R(T_2)$. The velocity is estimated from the phase difference between the two. The difference in PRT, $(T_2 - T_1)$, determines the unambiguous velocity, v_a , which is given by

$$v_a = \lambda/[4(T_2 - T_1)]; \quad T_1 < T_2. \quad (1)$$

If multiple-trip overlay is to be avoided, the unambiguous range

$$r_a = cT_1/2 \quad (2)$$

must be sufficiently large to encompass echoes from the farthest storms. Equations (1) and (2) suggest that the staggered PRT is equivalent to a uniform PRT = $(T_2 - T_1)$ for the unambiguous velocity and a uniform PRT = T_1 for the unambiguous range, and each can be selected independently. It is shown by Zrnic and Mahapatra (1985) that the standard error in the velocity estimate increases as the ratio $\kappa = T_1/T_2$ approaches unity, and a good choice is $\kappa = 2/3$. We use this value of κ in the rest of this paper.

In the absence of the ground clutter, one can use the pulse-pair method or the magnitude deconvolution method (Sachidananda and Zrnic 2000) to estimate the spectral parameters of the weather echoes. In the pulse pair method the velocity estimator based on the difference in phases of $R(T_1)$ and $R(T_2)$, (Eq. 7 of Zrnic and Mahapatra 1985), has a larger standard error than the uniform PRT pulse-pair velocity estimator, because it

uses the difference of two estimates. A better method is to take $R(T_1)$ for estimating an aliased velocity, and then use $R(T_2)$ for dealiasing. First, from the phases of $R(T_1)$ and $R(T_2)$, we compute two velocities v_1 and v_2 ,

$$\begin{aligned} v_1 &= -\lambda \arg\{R(T_1)\}/(4\pi T_1), \quad \text{and} \\ v_2 &= -\lambda \arg\{R(T_2)\}/(4\pi T_2). \end{aligned} \quad (3)$$

Now allowing for one-time aliases, the possible velocities from the first estimate are, v_1 , and $(v_1 + 2v_{a1})$ or $(v_1 - 2v_{a1})$, whichever falls inside the $\pm v_a$ interval, and from the second estimate we have v_2 and $(v_2 \pm 2v_{a2})$, where v_{a1} and v_{a2} are the unambiguous velocities corresponding to the PRT, T_1 and T_2 . Note that for $\kappa = 2/3$ (and typical v_{a1} and v_{a2} on 10-cm wavelength radars) it is sufficient to consider one time aliasing because the extended unambiguous velocity $v_a = 2v_{a1} = 3v_{a2}$. Of the aliased velocities only one value is common to both sets. This is the correct velocity, and can be selected after comparison. In general these values are estimates with a certain amount of error, hence we select the two values that are the closest and then choose the corresponding value from the first set. The values from the first set have lower variances than the ones from the second set because $T_1 < T_2$. This dealiasing procedure performs the best for $\kappa = 2/3$ because the difference between the estimated velocities, $|v_1 - v_2|$, is the largest whenever there is aliasing. For effective de-aliasing this separation must be larger than the standard error in the estimates. Thus, from the view point of large separation between these values, $\kappa = 2/3$ is the best choice.

In the magnitude deconvolution method (Sachidananda and Zrnic 2000), the staggered PRT sequence is converted to a uniform samples sequence of sampling period T_u by inserting zeros in place of missing samples. A discrete Fourier transform (DFT) of this sequence produces a spectrum with five replicas of the signal spectrum separated by 1/5th of the Nyquist interval (for $\kappa = 2/3$). Then the magnitude deconvolution is applied to reconstruct the original spectrum. This reconstruction is exact only for "narrow" spectra (spectral spread less than 1/5th of the Nyquist interval), but gives reasonably good estimates even if the spectra are slightly wider than specified by the "narrow" criterion. The spectral moments can then be estimated from this deconvolved spectrum.

We have tested these methods by simulations and have generated the error statistics. Figure 1 shows the standard error in the velocity estimates using the methods: 1) velocity from $R(T_1)$ and dealiasing from both $R(T_1)$ and $R(T_2)$, 2) velocity using magnitude deconvolution, and 3) velocity from $\arg [R(T_1)/R(T_2)]$. For comparison we have included the error estimates from $R(T_u)$, that is, uniform samples at intervals T_u . The dwell time for the three estimates is the same. The values are obtained using simulated time series and three different estimation algorithms on the same time series. The parameters of the simulation are indicated in the figure.

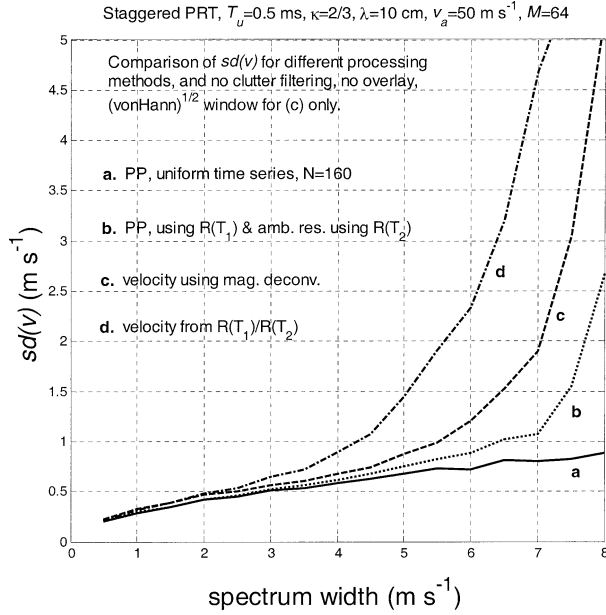


FIG. 1. Comparison of standard errors in the velocity estimates as a function of the spectrum width of the signal for different processing methods.

The signal-to-noise ratio is made large (>20 dB) so that the variance of the estimates is mainly due to the spectrum width and the sampling interval. It is clearly seen that method 1 gives the best estimate (curve “b” in the figure), followed by the other two, in that order. The deconvolution method (curve “c” in the figure) closely follows method 1 for spectrum width up to 4 m s^{-1} , and then the error starts increasing rapidly because of the overlap of the spectral replicas.

3. Ground clutter filtering

Here we briefly recapitulate the ground clutter filtering procedure given in Sachidananda and Zrnic (2000). The spectrum of the ground clutter is assumed to be narrow and centered on the zero Doppler velocity. The staggered PRT echo sample sequence is converted to a uniform sequence by inserting zeros in place of missing samples. Because the spectrum of the derived time series is the convolution of the code spectrum and the signal spectrum, it will have complex weighted replicas of the signal spectrum. The complex weights can be calculated from the code spectrum. In the clutter filtering procedure, we first find the complex clutter spectrum alone by projection and then subtract it from the spectrum to accomplish the filtering. Thus, we can retain some residual signal components in the spectral coefficients from which clutter is filtered.

To explain the clutter filtering we consider an example with parameters $\kappa = 2/3$, $M = 64$ for which $N = 160$. Select T_1 and T_2 such that they are integer multiples of some basic PRT T_u , so that $T_1 = n_1 T_u$, and $T_2 = n_2 T_u$,

where n_1 and n_2 are integers, and as we have already mentioned, $\kappa = 2/3$, $n_1 = 2$ and $n_2 = 3$ is assumed here. The code sequence is $c = [c_i, i = 1, 2, \dots, N] = [1010010100 \dots \text{etc.}]$, where 1s represent the positions of the staggered PRT samples and 0s represent the positions of missing samples in the uniform sample sequence. Let $g = (g_i, i = 1, 2, 3, \dots, M)$, be the alternately sampled (at time intervals T_1 and T_2) weather signal. We introduce zeros between g_i samples to produce a sequence $v = (v_i, i = 1, 2, \dots, N)$ of length $N = 5M/2$ with a uniform sampling period T_u . We call v the derived time series. We can write the sample sequence v as a product of the sequence c and e , where e is the complete time series of the signal sampled at T_u intervals,

$$v_i = c_i e_i; \quad i = 1, 2, 3, \dots, N. \quad (4)$$

Therefore, the spectrum of v is a circular convolution (\star) of the spectrum of the code c and the spectrum of the complete signal e ,

$$\text{DFT}(v) = \text{DFT}(c) \star \text{DFT}(e). \quad (5)$$

Equation (5) in matrix form is

$$\mathbf{V} = \mathbf{C}\mathbf{E}, \quad (6)$$

where \mathbf{V} and \mathbf{E} are $(N \times 1)$ column vectors of the DFT coefficients V_k and E_k of the corresponding time sequences, v and e , \mathbf{C} is the convolution matrix (size: $N \times N$) whose row vectors are cyclically shifted versions of coefficients C_k . Since the convolution matrix has only five nonzero coefficients in each column (or row), we can recast the matrix equation (6) in the form

$$\mathbf{V}_r = \mathbf{C}_r \mathbf{E}_r, \quad (7)$$

where subscript “r” is used to represent rearranged matrices. The convolution matrix, \mathbf{C} , is modified by deleting first all the rows containing zeros in the first column and then deleting all columns containing zeros in the first row, which reduces it to a 5×5 matrix, \mathbf{C}_r , and the other two matrices are rearranged as 5×32 matrices, row-wise. The Matrix \mathbf{C}_r is singular (its rank is 3), and its columns are normalized such that the sum of the magnitudes squared of the elements in each column is unity (This also normalizes the rows’ vectors). In the spectrum ($E_k, k = 1, 2, 3, \dots, N$) of the complete time series, the clutter is confined to the first and last few coefficients ($k = 1, 2, \dots, q$ and $N - q - 2, \dots, N$). This is because the first coefficients correspond to positive components and the last to negative in the Doppler Spectrum. Therefore, the matrix \mathbf{V}_r would have clutter power spread over the first few and the last few columns.

The clutter from the first few columns of \mathbf{V}_r is removed by subtracting the projection of each column onto the first column of \mathbf{C}_r times the first column of \mathbf{C}_r . Similarly, the clutter from the last few columns is removed using the last column vector of \mathbf{C}_r in place of

the first. This complete operation can be written in matrix notation as

$$\mathbf{V}_f = \mathbf{V}_r - \mathbf{C}_{f1}\mathbf{V}_r\mathbf{I}_{f1} - \mathbf{C}_{f2}\mathbf{V}_r\mathbf{I}_{f2}, \quad (8)$$

where \mathbf{C}_{f1} and \mathbf{C}_{f2} are the clutter filter matrices, and \mathbf{I}_{f1} and \mathbf{I}_{f2} are matrices that select the columns to be filtered. These are given by

$$\mathbf{C}_{f1} = \mathbf{C}_1\mathbf{C}_1^* \quad (9a)$$

$$\mathbf{C}_{f2} = \mathbf{C}_5\mathbf{C}_5^*, \quad (9b)$$

where \mathbf{C}_1 is the first column vector of \mathbf{C}_r , \mathbf{C}_5 is the last column vector (fifth column for $\kappa = 2/3$) of \mathbf{C}_r , the superscript “ t^* ” indicates complex conjugate transpose. The matrix \mathbf{I}_{f1} is a $M/2 \times M/2$ diagonal matrix with diagonal elements equal to 1 for the first q elements and 0 for the rest. Similarly, the matrix \mathbf{I}_{f2} is a $M/2 \times M/2$ diagonal matrix with last $(q - 1)$ elements unity and the rest zeros. For example, the diagonals of the matrices for $q = 4$ are

$$\begin{aligned} \text{diag}\{\mathbf{I}_{f1}\} &= [11110000 \cdots 000], \quad \text{and} \\ \text{diag}\{\mathbf{I}_{f2}\} &= [0000 \cdots 000111]. \end{aligned} \quad (10)$$

Note that $(2q - 1) = n_c$ is the clutter filter width in terms of the number of spectral coefficients. Hence, the first four ones in (10) correspond to 0th to 3rd spectral coefficients and the last three ones in (10) are the three coefficients closest to 0th coefficient on the negative side. Here, \mathbf{V}_f is the matrix of signal spectrum after clutter filtering. This filtering procedure does not delete all the signal power present in the coefficients from which clutter is filtered. Of course, if the signal velocity is also near zero it cannot be distinguished from the clutter and hence will be deleted completely. (Note that in this case the bias is small because the velocity itself is near zero and the bias is towards zero velocity.) For signals with mean velocity other than near zero, a part of the signal power is retained, but is reshuffled in amplitude and phase in the clutter filtering process. This produces a bias in the velocity estimate, which can be eliminated if we can reconstruct the original signal from the residual signal power. The original signal coefficients can be restored completely in the complex domain, or alternately, we can recover only the magnitudes, which is sufficient to estimate the spectral moments. The second procedure involves less computation. Both procedures require the approximate mean velocity of the signal. In the next section we explain both procedures for restoring the lost signal. To obtain the approximate mean velocity estimate we use magnitude deconvolution after filtering the ground clutter. Magnitude deconvolution is applied to the rearranged matrix directly, and is given by the equation

$$\mathbf{E}_r = [\text{abs}(\mathbf{C}_r)]^{-1} \text{abs}(\mathbf{V}_f). \quad (11)$$

The magnitude spectrum $\text{abs}(\mathbf{E}_r)$ is rearranged in a column matrix \mathbf{E}_s . The autocorrelation $R(T_u)$ is calculated from the magnitude coefficients of \mathbf{E}_s , and the initial

approximate velocity estimate is obtained from the phase of $R(T_u)$. We shall use this initial velocity estimate (referred to as *initial* velocity estimate later) information in removing the bias. An example of the velocity estimates and the associated bias due to the clutter filtering on simulated time series is in Figs. 5 and 6 of Sachidananda and Zrnic (2000). It is significant that there is a wavy kind of bias in the velocity estimate, and in regions where the signal and the clutter spectra overlap (i.e., at 0 , $\pm 2v_a/5$, and $\pm 4v_a/5$), there is an increase in the standard error, but the bias is zero. The bias is maximum (positive or negative) in between two of these variance peaks because the clutter filtering removes a part of the signal from one side of the spectrum asymmetrically, which produces the bias.

4. Bias removal procedure

It is mentioned in the previous section that the clutter filtering from a column of the \mathbf{V}_r alters the relative amplitudes of the signal components present in the column, thus, preventing it from deconvolving into a single signal component in \mathbf{V}_f . A very interesting feature of \mathbf{V}_f is that the amplitudes of all the elements of the column vector from which clutter is filtered are modified such that after magnitude deconvolution the amplitudes of all elements of the column vector are the same (see also the appendix). Furthermore, this amplitude bears a fixed relation to the actual signal component present in the vector. This relation can be obtained by performing the matrix operations corresponding to the clutter filtering and magnitude deconvolution on each of the unit column vectors \mathbf{C}_1 to \mathbf{C}_5 and is given by

$$\xi_k = 1/\mathbf{D}_k(1), \quad (12)$$

where $\mathbf{D}_k(1)$ is the first element of column matrix \mathbf{D}_k given by

$$\begin{aligned} \mathbf{D}_k &= [\text{abs}(\mathbf{C}_r)]^{-1} \text{abs}[\mathbf{C}_k - \mathbf{C}_1^*\mathbf{C}_k\mathbf{C}_1]; \\ k &= 1, 2, \dots, (n_1 + n_2). \end{aligned} \quad (13)$$

For a given k the magnitudes of the five elements of \mathbf{D}_k are the same (can be positive or negative), and the first element is always positive, hence we have used the first element in Eq. (12). Furthermore, \mathbf{C}_r is the rearranged code matrix defined earlier, \mathbf{C}_k is the k th column vector of \mathbf{C}_r , and ξ_k is the ratio of the actual signal amplitude to the amplitude after magnitude deconvolution for the k th velocity region. There are three velocity regions; the regions (1), (2), and (3) are $|v| < v_a/5$, $v_a/5 < |v| < 3v_a/5$, and $3v_a/5 < |v| < v_a$, respectively, for $\kappa = 2/3$. The ξ_k values are symmetric with respect to the zero velocity; that is, the positive and negative velocities have the same value (except for the sign which is discarded because we are working in the magnitude domain), therefore only the first three values are taken for $\kappa = 2/3$ [For negative velocity region replace \mathbf{C}_1 with \mathbf{C}_5 in Eq. (13).] Note that $\xi_1 \rightarrow \infty$, hence cannot be used

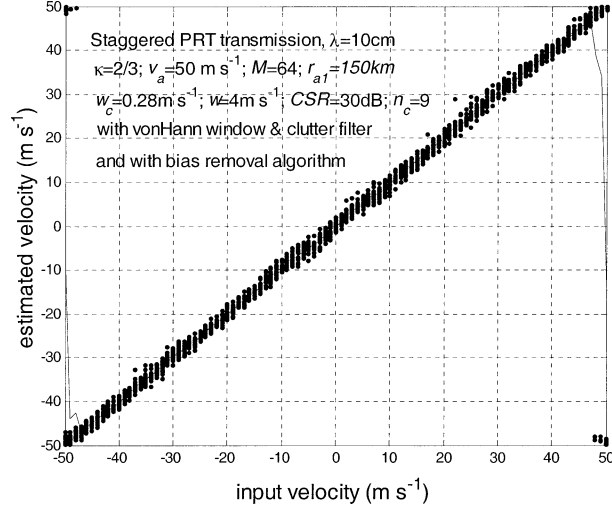


FIG. 2. The estimated velocity vs the input velocity after the clutter filtering and bias correction algorithm. The parameters used in the simulation are indicated.

for signal amplitude correction in region $|v| < v_a/5$, and is set to unity.

To restore the true signal amplitude in the filtered columns of \mathbf{V}_f , we first identify the row in which signal component is to be restored based on the *initial* velocity estimate, and multiply that coefficient by ξ_k , for region 2 and 3. The rest of the elements of that column are set to zero. For region 1, this particular row elements, are replaced by $(q + 1)$ th element value for columns 1 to q , and $(M/2 - q + 1)$ th value for columns $(M/2 - q + 2)$ to $M/2$. This, of course, is an approximation for want of an accurate ξ . If the clutter and signal vectors overlap in this region the signal would be completely removed while filtering the clutter. Therefore, we take the signal amplitude from the adjacent coefficient from which clutter is not filtered [e.g., $(q + 1)$ th column] and insert this value as an approximate signal amplitude. This, of course, is not the best choice, but is the simplest option. The bias removal is not exact for region 1, but is reasonably good for most applications. This procedure is carried out for the columns from which clutter is filtered. In matrix notation this operation is represented by

$$\mathbf{E}_s^c = \mathbf{E}_s \cdot \mathbf{I}_1 + \mathbf{E}_s^m \cdot \mathbf{I}_2 \cdot \mathbf{I}_v \cdot \mathbf{Z}, \quad (14)$$

where \mathbf{E}_s^c is the corrected spectrum, and \mathbf{E}_s^m is the modified spectrum in which the first q elements of \mathbf{E}_s are replaced by $(q + 1)$ th element and the last $(q - 1)$ elements are replaced by the $(N - q + 1)$ th element. This modification is made to take care of the correction in region 1. The dot (\cdot) symbolizes an element by element multiplication operation of the two columns, like the ($*$) operation in MATLAB). The other column matrices used in (14), \mathbf{I}_1 , \mathbf{I}_2 , \mathbf{I}_v and \mathbf{Z} are defined by

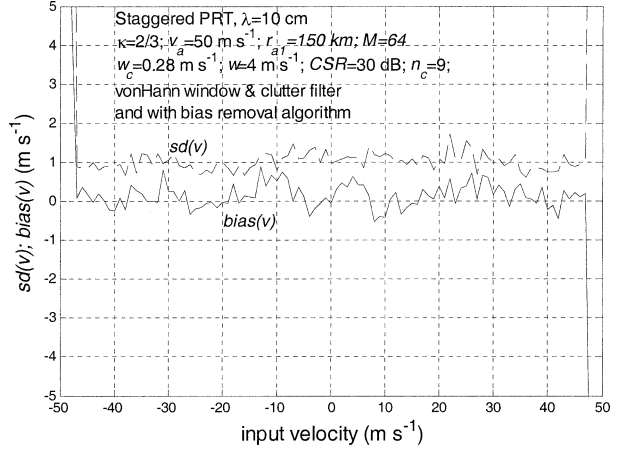


FIG. 3. Bias and standard error in the velocity estimates using the staggered PRT clutter filtering and bias correction algorithm. The simulation parameters are the same as in Fig. 2.

$$\mathbf{I}_2 = [\text{diag}(\mathbf{I}_{f_1}) + \text{diag}(\mathbf{I}_{f_2}), \dots \text{repeat } (n_1 + n_2) \text{ times}]', \quad (15)$$

$$\mathbf{I}_1 = \text{complement of } \mathbf{I}_2, \quad (\text{interchange zeros and ones}), \quad (16)$$

$$\mathbf{I}_v = [000 \dots 001111 \dots 1110000 \dots] \quad (17)$$

[N elements with $N/(n_1 + n_2)$ 1s placed such that they are centered on the mean velocity coefficient, the rest are all 0s], and

$$\mathbf{Z} = [1111 \dots, \xi_2, \xi_2, \xi_2, \dots, \xi_3, \xi_3, \xi_3, \dots, \xi_2, \xi_2, \xi_2, \dots, 111 \dots]'. \quad (18)$$

The parameters, ξ_2 , ξ_3 , etc., are the correction coefficients for the velocity regions 2, 3, etc. The region 1 correction coefficient is set to unity (actually $\xi_1 \rightarrow \infty$) because it is not used in the correction scheme. The velocity scale corresponding to the spectral coefficients 1 to N is from 0 to $-v_a$, and $+v_a$ to 0; therefore, the first $N/2(n_1 + n_2)$ and the last $N/2(n_1 + n_2)$ coefficients are 1s representing region 1. The next $N/(n_1 + n_2)$ coefficients correspond to the region 2 and so on up to the center, and then the same coefficients repeat in the reverse order up to the end. The values are $\xi_2 = 1.105$ and $\xi_3 = 1.789$ for $\kappa = 2/3$.

Figure 2 shows the velocity recovery for $\kappa = 2/3$ and $v_a = 50 \text{ m s}^{-1}$, and in Fig. 3 is the plot of bias error and standard deviation of the velocity estimate, $\text{sd}(v)$. Compare these two figures with Figs. 5 and 6 of Sachidananda and Zrnic (2000), which are for the same simulation parameters before bias correction. It can be observed that the bias error is nearly zero for the entire $\pm v_a$ interval. The large error at the extremities is caused by velocity aliasing. The procedure also removes the bias error in the spectrum width estimate. Figure 4 shows the bias and standard error in the width estimate before the bias correction. The input width is 4 m s^{-1} ,

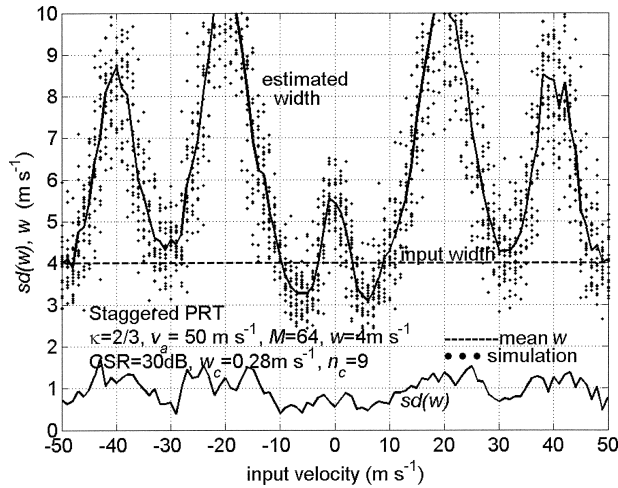


FIG. 4. The estimated spectrum width and its standard error as a function of the input velocity after the clutter filtering and without the bias correction.

and the input velocity is varied over the entire Nyquist interval. The dots represent the simulation points. For the same set of simulation parameters, the estimated width after the bias removal is shown in Fig. 5, which clearly indicates the effectiveness of the bias removal.

Simulation results show that for $CSR > 40$ dB, which requires wide clutter filter, the bias error is too large to be completely removed over the entire velocity interval. There are some outliers, especially the regions where the clutter and signal overlap. That is also where the bias correction is further impeded because the algorithm uses the *initial* velocity estimate (which has a large variance) to determine the matrix \mathbf{I}_v (17).

For signals with larger spectrum width ($w > 6$ m s^{-1}), the reconstruction of the spectra is not accurate because of the overlap, hence, there is an increase in the $sd(v)$. The method is applicable to any κ , but the code and convolution matrix differ, and so does the quality of the results. We have tried with $\kappa = 3/4$ and it works fine but with a larger standard error. The increase in standard error is not due to the increased spectral overlap. It is not proper to compare the $\kappa = 2/3$ and $\kappa = 3/4$ with same T_u (basic sampling period), rather these should be compared for the same $(T_1 + T_2)$ and dwell time. If $(T_1 + T_2)$ is kept the same we find the unambiguous velocity is increased by a factor 7/5 for $\kappa = 3/4$, and the spectrum contains seven replicas in place of 5 for $\kappa = 2/3$. Thus, for a given spectrum width the spectral overlap is the same but v_a and r_{a1} change. The increase in the error is mainly due to less information available in the case of $\kappa = 3/4$ (two samples out of seven against two out of five for $\kappa = 2/3$).

5. Restoration of complex spectral coefficient

Let us start with Eq. (7), $\mathbf{V}_r = \mathbf{C}_r \mathbf{E}_r$, where \mathbf{E}_r is the signal plus the clutter spectrum. Assume that the ground

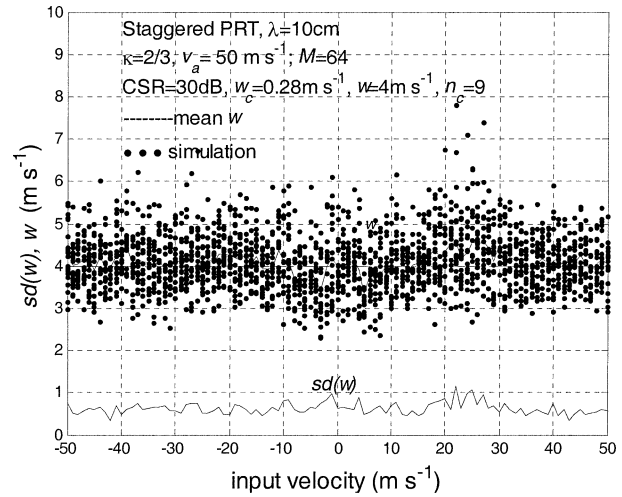


FIG. 5. The estimated spectrum width and its standard error as a function of the input velocity after the bias correction. The simulation parameters are the same as in Fig. 4.

clutter spectrum is centered at zero Doppler and the signal spectrum is “narrow” (the spread of the nonzero spectral coefficients is limited to 1/5th of the $\pm v_a$ interval for $\kappa = 2/3$). With this assumption, the first few coefficients in the first row and last few coefficients in the last row of \mathbf{E}_r have ground clutter. The nonzero signal coefficients are spread over only $N/5$ contiguous coefficients row wise; the mean velocity of the signal determines the position. Thus in any column of \mathbf{E}_r , a maximum of two coefficients can be nonzero. Now, the convolution operation (7) spreads the clutter and the signal power (present in each column of \mathbf{E}_r) into all the coefficients of the same column of \mathbf{V}_r . There is no shifting of the power from one column to another. Therefore, it is sufficient to consider one column of \mathbf{V}_r and \mathbf{E}_r to understand the signal restoration procedure. Let the first column of \mathbf{E}_r be $\mathbf{E}_1 = [a, 0, 0, b, 0]^T$, where a is the clutter coefficient, and b is the signal coefficient; both complex. After the convolution, the first column of \mathbf{V}_r , \mathbf{A} is given by

$$\mathbf{A} = \mathbf{C}_r \mathbf{E}_1 = a \mathbf{C}_1 + b \mathbf{C}_4. \quad (19)$$

After clutter filtering (9) the first column of \mathbf{V}_f can be written as

$$\mathbf{B} = \mathbf{A} - \mathbf{C}_1^* \mathbf{A} \mathbf{C}_1. \quad (20)$$

Substituting for \mathbf{A} and simplifying we can reduce (20) to

$$\mathbf{B} = b(\mathbf{C}_4 - \mathbf{C}_1^* \mathbf{C}_4 \mathbf{C}_1). \quad (21)$$

Note that the clutter coefficient a is completely deleted by the clutter filtering, but the signal component b is multiplied by a complex known vector. To restore the signal vector $b \mathbf{C}_4$ present in \mathbf{A} , we carry out the matrix operation

$$b \mathbf{C}_4 = (\mathbf{C}_4^* \mathbf{B} \mathbf{C}_4) / (1 - |\mathbf{C}_1^* \mathbf{C}_4|). \quad (22)$$

This procedure is applied to the first few columns of \mathbf{V}_f from which clutter has been filtered.

In this illustration we have assumed that the signal coefficient is in the fourth position in \mathbf{V}_1 . In general the position of the signal coefficient can be any one of the five, hence a general expression becomes

$$b\mathbf{C}_k = (\mathbf{C}_k^* \mathbf{B} \mathbf{C}_k) / (1 - |\mathbf{C}_k^* \mathbf{C}_k|^2), \quad (23)$$

where k is the position of the signal coefficient which is determined from the *initial* velocity estimate. For the last few columns of \mathbf{V}_f the clutter coefficient is in the last row, hence \mathbf{C}_1 is replaced by \mathbf{C}_5 in (23) while restoring the signal in these columns. Note that in (23) the denominator is zero if $k = 1$, which corresponds to the signal having near-zero Doppler. The signal is completely filtered out, and the numerator also would be zero in this case. In the actual radar time series processing, however, the numerator would not be zero because the signal spread is not “narrow” in the strict sense. Thus, we cannot restore the signal if the Doppler is near zero as in the previous method.

If the assumption of “narrow” spectra is strictly valid then both the methods of signal restoration are exact, and give the same spectral moment estimates. However, if the spectra are not “narrow” the two methods differ in performance to some extent. The magnitude restoration performs slightly better than the complex domain restoration in the presence of overlapping spectral replicas, and also requires less computation.

6. Effect of window function on clutter filter performance

In the absence of clutter it is advantageous to use the autocovariance processing as mentioned earlier in section 2a. It is also well known that autocovariance processing gives estimates with lowest standard error if window weighting is not used (Sachidananda et al. 2000). Further, it leads to less computation compared to the spectral domain processing. However, if clutter filtering is needed, application of window and spectral processing becomes necessary. In this section we shall discuss the effect of window function on the recovery of the spectral moments of the weather signal in the presence of large ground clutter.

The ground clutter is generally present in lower elevation scans, typically in the first 20 km from the radar. At elevations higher than about 5° the ground clutter is not a serious problem. The Weather Surveillance Radar-1988 Doppler (WSR-88D) specifies 50 dB rejection for the ground clutter with a spectrum width of 0.28 m s^{-1} centered on zero Doppler (this specification is for scans at 0.5° and 1.45°). We use this width for the ground clutter in our simulation study, and specify clutter-to-signal ratio (CSR) as a parameter rather than the clutter rejection. We adopt this notation because our ultimate aim is to recover the spectral moments of the weather echo, and to achieve this, it is sufficient to filter enough

clutter power to get a decent signal-to residual clutter ratio [equivalent to signal-noise-ratio (SNR)] so that the spectral moment estimates are accurate. The amount of filtering required depends on the CSR. Further, the clutter suppression ratio α , defined as the ratio of the total clutter power to the residual clutter power after filtering, expressed in dB units, is a function of the filter width; hence, any suppression can be obtained by suitably choosing the filter width. But this does not guarantee recovery of spectral moments of the weather signal because there is an upper limit for the filter width beyond which the velocity cannot be recovered irrespective of the CSR. There is always an optimum clutter filter width for a given CSR and a clutter spectrum width. If the clutter filter width is adjusted in the staggered PRT decoding algorithm based on an a priori knowledge of the CSR, the performance of the algorithm can be optimized. It is obvious that the residual clutter power is spread throughout the spectrum, hence, can be treated as noise. Thus, the SNR after filtering the ground clutter is equal to $(\alpha - \text{CSR})$ dB, neglecting the noise power (or assuming the noise power to be very small compared to the residual clutter power), and that the signal and clutter spectra are not overlapping. This has to be better than 10 dB to recover velocity of the weather echo with a good accuracy.

The window function and the number of staggered PRT samples available for processing play important roles in the clutter filter performance, because, the suppression ratio is a strong function of these two parameters. An appropriate choice of window function can limit the spread of the spectral powers, thus enabling a better clutter rejection with narrower clutter filter width. There are several window functions available in the literature, but we have chosen to examine the (von Hann)^{*n*} window because it captures most of the effects that can be obtained with other windows, especially that of suppressing the side lobes. By selecting a different exponent, n , the window taper or the side lobe level can be controlled; larger the n lower is the side lobe level, but with a wider main lobe. For a given n there is an upper limit for the clutter suppression ratio α . The upper limit also depends on the number of samples M . Figure 6 illustrates the clutter suppression ratio versus the normalized clutter filter width, $w_f/2v_a$, for different windows and two different values of M . The data is obtained from a large number of simulations using Gaussian shaped clutter spectra, and their mean values are plotted. The filter widths are discrete because the filter is implemented in the spectral domain where only integer number of coefficients can be deleted (only odd numbers are used for n_e , the filter width in terms of the number of coefficients). The inherent rectangular window spreads clutter power across the spectrum giving a low α . Higher order windows (larger n) allow better clutter suppression, but need a wider filter. There is a signal power loss associated with window that increases the standard error in the mean velocity estimate. Note that

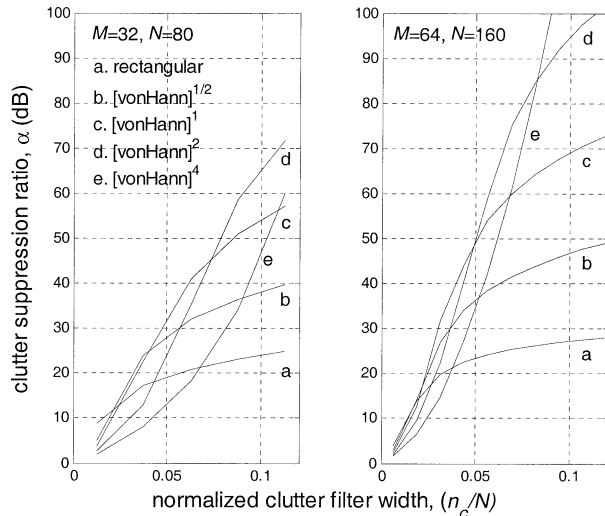


FIG. 6. Clutter suppression ratio as a function of the normalized clutter filter width with window function as a parameter.

for the signal velocity estimation, it is sufficient to make $(\alpha - \text{CSR}) > 10$ dB. Therefore, the exponent n and the clutter filter width have to be optimized for a given CSR. For a given N , the exponent n must be selected such that we can achieve an $\alpha > (\text{CSR} + 10)$ dB. A higher n will allow a lower filter width, but with associated signal loss. The signal power loss can be computed from the weighting function directly as 4.23, 5.67, and 7.03 dB for $n = 1, 2,$ and 4 , respectively.

It is also seen from Fig. 6 that α is very sensitive to the number of samples M (or N). Thus, increasing the number of samples would allow a higher α for a given window. We observe that higher the order of the window, more samples at both ends of the sequence are suppressed, and do not significantly contribute to the estimate. Although the number of samples available from a radar is limited by the allowable dwell time, we can increase N by simply adding zeros at both ends of the sequence, and then apply the window to the extended sequence. Higher the order of the window, more zeros can be added. If we use a criterion that the side lobe level of the spectra should not be altered significantly by adding zeros, the number of zeros that can be added are about 14%, 33%, and 76% of the available samples for $n = 1, 2,$ and 4 , respectively. This is calculated from the window weights and verified using simulation. Further, it reduces the signal loss due to the weighting to about 3.5 dB in all three cases, hence allows us to achieve a higher α without sacrifice of the estimate error. This is significant and therefore worth implementing on a radar. Simulation results (not presented here) show that using a (von Hann)⁴ window and 76% lengthened sequence by adding zeros, allows accurate velocity recovery for a CSR as high as 50 dB with 50 staggered PRT samples.

A special situation arises in the clutter filtering if the signal velocity straddles $0, \pm 2v_d/5,$ or $\pm 4v_d/5,$ for $\kappa =$

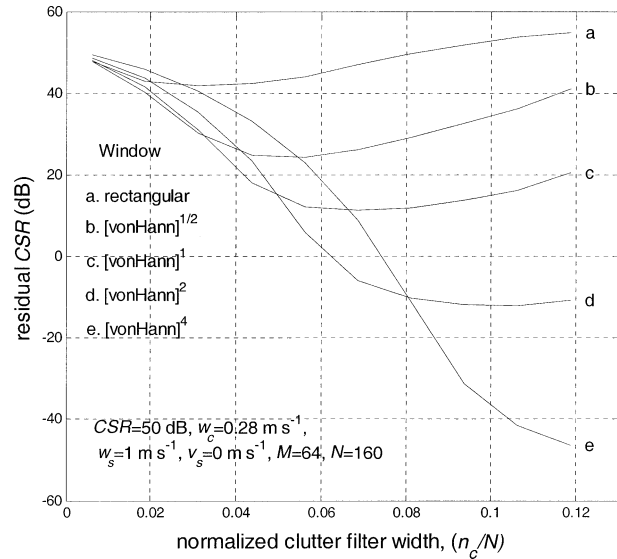


FIG. 7. Residual CSR vs the clutter filter width for different window functions.

$2/3,$ and the signal spectrum width is very narrow. In this specific case, the SNR after the ground clutter filtering is not equal to $(\alpha - \text{CSR})$ dB for the *initial* approximate velocity estimation, because the signal is also filtered along with the clutter. The above formula is valid only if the signal and clutter spectra do not overlap. If the signal and clutter spectra overlap, the ability to achieve a $\text{SNR} > 0$ dB after filtering depends on the relative spectrum widths of the clutter and the signal, and the manner in which the signal and clutter power fall as a function of the clutter filter width. For the velocity recovery, the first condition is that the signal spectrum width must be larger than the clutter spectrum width, so that the rate at which the residual signal decreases as a function of the clutter filter width is slower than the rate at which the clutter signal decreases. Only under this condition the residual SNR increases as a function of the clutter filter width, and can become greater than zero for sufficiently large width.

The window function is very critical in achieving residual $\text{SNR} > 0,$ because it changes side lobe structure of the spectrum. Figure 7 shows the residual CSR after the clutter filtering using different n values for the (von Hann) ^{n} windows. Note that SNR after clutter filtering is the inverse of the residual CSR (or negative of the residual CSR in dB.) The overlapping signal spectrum width is assumed to be $1 \text{ m s}^{-1},$ and the clutter spectrum width is equal to $0.28 \text{ m s}^{-1}, \text{ CSR} = 50 \text{ dB}.$ The weather signal and clutter spectra are simulated, and different clutter filter widths are used to compute the residual CSR. The number of samples $N = 160 (M = 64),$ but it should be noted that the achievable residual SNR also depends on the number of samples. Note that the residual CSR initially decreases and then starts increasing. Further, observe from the figure that a minimum $n =$

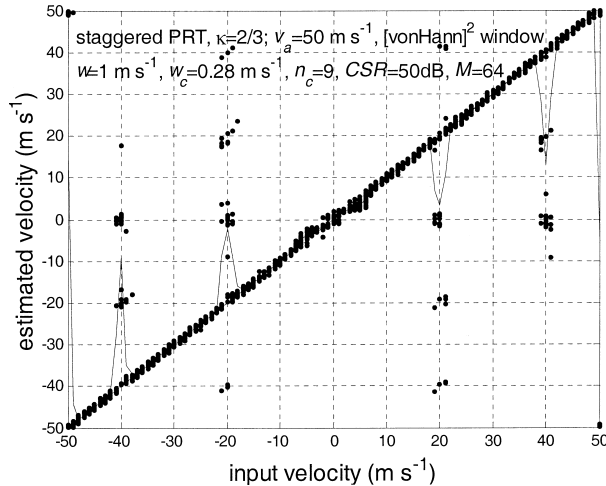


FIG. 8. Results of the velocity recovery simulations for a CSR = 50 dB using (von Hann)² window. The estimated velocity from simulated time series is plotted against the input velocity.

2 is required to achieve a residual CSR < 0 dB and that $n = 4$ allows a better CSR than is possible with $n = 2$, but with a slightly wider clutter filter width. The results of a study using staggered PRT processing on a simulated time series with $w = 1 \text{ m s}^{-1}$ and a CSR = 50 dB ($w_c = 0.28 \text{ m s}^{-1}$) are in Figs. 8 and 9. It can be seen that whenever the signal and clutter spectra overlap (happens for $v = 0, \pm 2v_a/5$, or $\pm 4v_a/5$), filtering with the (von Hann)² cannot recover velocity effectively but with (von Hann)⁴ window the recovery is satisfactory. Thus, it can be concluded that for large CSR and narrow signal spectrum it is advantageous to use (von Hann)⁴ window. For lower CSR or wider signal spectra (von Hann)² is generally sufficient.

7. Noise considerations

The effect of noise or the signal-to-noise ratio on the spectral parameter estimates is very well documented in Doviak and Zrnic (1993). Generally the weather signals have a good SNR (>20 dB) for most regions except where the reflectivity is very low or for echoes from large ranges. A SNR > 30 dB is used in all simulations. For SNR > 20 dB the variance in the estimates is mostly due to the nature of the weather signal itself and it is a function of spectrum width and sampling interval. For SNR < 20 dB however the noise contribution starts increasing but the increase can be tolerated up to about SNR = 3 dB.

The ground clutter is generally limited to close ranges (<20 km) and for these ranges the SNR is generally much larger than 20 dB. Hence, SNR is not a consideration in the clutter filtering algorithm. However, a matter of more concern is the CSR and the residual clutter power after filtering. The residual clutter to signal ratio is similar to the noise and certainly affects the estimates as in the result presented herein. An additional source

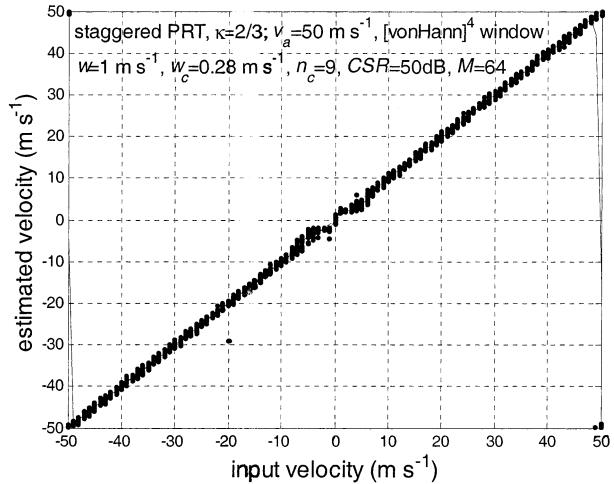


FIG. 9. Results of simulations with the same parameters as in Fig. 8, but (von Hann)⁴ window. The estimated velocity from simulated time series is plotted against the input velocity.

of error is the magnitude deconvolution because it reconstructs exactly only spectra that are within 1/5th of the full interval. For broader spectra there will be overlap of the spectral replicas, and the reconstruction is not exact. Any modification of the spectrum obviously leads to an increase in the estimate variance (Fig. 1), and the magnitude deconvolution also increases the error for larger width signals.

8. Conclusions

This paper presents enhancements to our earlier clutter filtering algorithm for the staggered PRT sequences, which had some bias in the spectral moment estimates. An alternative pulse pair estimator of mean velocity in the absence of clutter is discussed, which performs better than other methods. Simulation results indicate that this is the preferred procedure if there is no clutter, because it avoids FFT processing. Simple pulse pair estimator and some comparison is all that is required. However, if the ground clutter is present the spectral processing becomes necessary. Of the two bias removal algorithms explained in the paper, the magnitude only recovery is recommended. It performs better and also requires less computation. The technique is shown to remove effectively the biases in both velocity and spectrum width estimates.

In the presence of the ground clutter, selection of the window function and the clutter filter width are important to recover the spectral moments. It is shown that a higher order window that has low side lobes allows recovery of spectral moments of weak signals (large CSR). Further, it is suggested that the loss associated with window weighting (and the resulting increase in standard error in the estimates) can be mostly overcome by processing an extended time series obtained by adding a sequence of zeros of appropriate length.

Acknowledgments. The authors wish to thank Jim Evans of Lincoln Laboratory for suggesting alternative possibilities for velocity estimation. An anonymous reviewer pointed out errors that prevented correct replication of our results. Part of this work was supported by the Radar Operations Center of the NWS.

APPENDIX

Effects of Filtering on the Signal Spectral Component

The bias in the velocity estimate is due to the loss of spectral components of the signal caused by the clutter filtering procedure. The bias is corrected by restoring the lost signal components to their original values. To illustrate this procedure let us take an example in which the number of staggered PRT samples is $M = 64$ (uniform sequence length, $N = 160$). Assume that the weather echo signal has one Doppler coefficient of unit amplitude at a DFT coefficient number 34 and the ground clutter has one coefficient at number 2, with an amplitude of 100 (40 dB higher than the signal). Because the staggered PRT spectrum is a convolution of the (signal + clutter) spectrum with the code spectrum (4), which has only 5 nonzero coefficients separated by 32 coefficients, (in this case the code is: 1010010100...etc.), the clutter coefficient will spread to 5 DFT positions (2, 34, 66, 98, and 130). Similarly, the signal power is spread over these same coefficients, although the original signal is at location 34. The amplitudes and phases of these coefficients are listed in Table A1.

The same data (magnitude only) is plotted in Figs. A1a–f. It may be noted from the table that the convolution operation preserves the phase of the original coefficient (0° of coefficient 2 for clutter, and of coefficient 34 for signal). The spectrum of the staggered PRT signal is the sum of the spectra in Figs. A1c and A1d. The clutter filtering (9) removes all the clutter power from the five locations (2, 34, 66, 98, 130). A simple filtering would have deleted all the power from the five coefficients, but the present procedure leaves residual signal power at four of the locations (34, 66, 98, 130). This spectrum when processed through magnitude deconvolution (12), produces a constant magnitude at all the five locations (Fig. A1f). It can be shown that this magnitude is a specific fraction of the original signal that

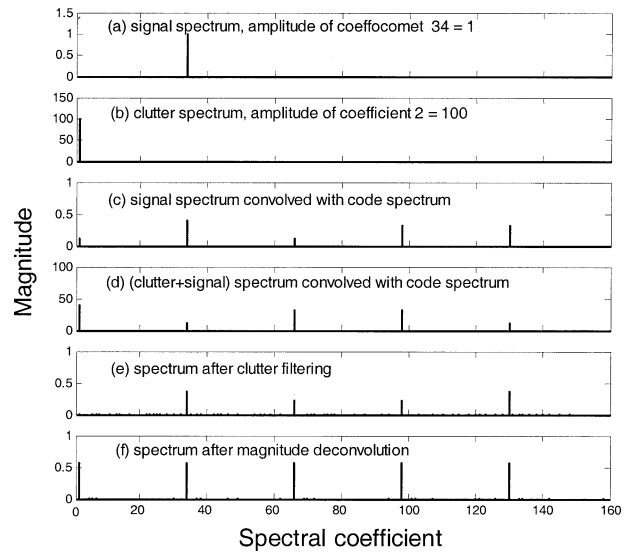


FIG. A1. Illustration of the bias correction procedure with a single clutter and a single signal spectral component. The clutter component is at the second spectral coefficient, the signal at location 32. Spectra of these components, convolved spectra, spectrum after clutter filtering, and spectrum after magnitude deconvolution are plotted in (a)–(f).

we have started with in Fig. A1a (unit amplitude). Hence, multiplying by the known constant (ξ) we can restore the signal amplitude. Further, of the five, only one is the original location, and the other coefficients are discarded. To find out which is the original location, we rely on the initial estimate of the velocity obtained before bias correction. Because the clutter spectrum width is much smaller than the signal spread, clutter filtering affects only some of the signal coefficients and the rest contribute to the approximate initial estimate of the mean velocity. If the bias is less than $1/5$ th of the Nyquist interval, the locations of the original signal component can be determined.

REFERENCES

- Doviak, R. J., and D. S. Zrnic, 1993: *Doppler Radar and Weather Observations*. Academic Press, 562 pp.
 Sachidananda, M., and D. S. Zrnic, 2000: Clutter filtering and spectral moment estimation for Doppler weather radars using stag-

TABLE A1. DFT coefficients at different steps of clutter filtering.

Coefficient no.	2	34	66	98	130
(a) Signal	0	1	0	0	0
(b) Clutter	100	0	0	0	0
(c) Signal*code: Magnitude	0.1236	0.4000	0.1236	0.3236	0.3236
Phase ($^\circ$)	72.0	0.0	-72.0	36.0	-36.0
(d) Clutter*code: Magnitude	40.0384	12.4901	32.3227	32.4621	12.2645
Phase ($^\circ$)	0.0	-72.0	36.0	-36.0	72.0
(e) After clutter filter	0.0000	0.3618	0.2236	0.2236	0.3618
(f) Magnitude deconv.	0.5721	0.5721	0.5721	0.5721	0.5721

- gered pulse repetition time. *J. Atmos. Oceanic Technol.*, **17**, 323–331.
- , —, and R. J. Doviak, 2000: Signal design and processing techniques for WSR-88D ambiguity resolution, Part-4. National Severe Storms Laboratory.
- Sirmans, D., D. Zrnic, and B. Bumgarner, 1976: Extension of maximum unambiguous Doppler velocity by use of two sampling rates. Preprints, *17th Conf. on Radar Meteorology*, Seattle, WA, Amer. Meteor. Soc., 23–28.
- Zrnic, D. S., and P. Mahapatra, 1985: Two methods of ambiguity resolution in pulsed Doppler weather radars. *IEEE Trans. Aerosp. Electr. Syst.*, **21**, 470–483.